Optics Letters

Forward Brillouin scattering acoustic impedance sensor using thin polyimide-coated fiber

Desmond M. Chow* and Luc Thévenaz

EPFL Swiss Federal Institute of Technology, Institute of Electrical Engineering, SCI STI LT, Station 11, CH-1015 Lausanne, Switzerland
**Corresponding author: desmond.chow@epfl.ch*

Received 6 August 2018; revised 4 October 2018; accepted 9 October 2018; posted 9 October 2018 (Doc. ID 341756); published 31 October 2018

The standard single-mode fiber has been demonstrated as an optomechanical sensor recently to measure the acoustic impedances of surrounding liquids by means of the generation and detection of forward-stimulated Brillouin scattering (FSBS). FSBS allows the mechanical properties of an external material to be probed directly through the interaction of guided light and transverse sound waves that occurs entirely inside the fiber structure. In this technique, having a low-loss interface between the fiber bulk and the external medium is essential for precise measurement; however, it leads to the necessary but impractical removal of the thick polymer fiber coating in most reported methods. Here, we use a commercially available 80-µm-diameter optical fiber coated with a 8-µm-thick polyimide coating layer to measure the acoustic impedances of the surrounding liquids, showing accurate measurement results while retaining the mechanical strength of the fiber.

https://doi.org/10.1364/OL.43.005467

Opto-acoustic interactions in optical fiber is a fascinating discipline that inspires a broad range of sensors, such as those based on stimulated Brillouin scattering (SBS), which has been widely used to perform distributed strain and temperature measurements [1–3]. Recently, another class of opto-acoustic interaction in optical fibers—forward-stimulated Brillouin scattering (FSBS) has been exploited to measure the acoustic impedance of liquid surrounding a standard optical fiber [4–6]. FSBS is also known as guided acoustic wave Brillouin scattering (GAWBS) [7]. This effect involves optically stimulating the transverse acoustic waves in an optical fiber through electrostriction. Because of the circular fiber's cross section at the cladding exterior boundary, the acoustic waves are reflected and confined inside the disc-shaped transversal cavity, giving rise to eigenmodes with resonant frequencies in the radio frequency range. The difference of acoustic impedance between the fiber material and the external medium determines the acoustic reflectivity at the fiber's boundary and can be detected optically through measuring the decay rate [4] or linewidth [5] of the FSBS resonances. Taking advantage of the long length of optical fiber, distributed FSBS acoustic impedance sensing has also been demonstrated recently [8,9], indicating the potential of using the transverse acoustic wave in mapping the external environment.

However, most reported implementations of FSBS-based acoustic impedance sensors rely on stripping away the fiber's acrylate coating that shows high acoustic loss to facilitate direct contact between the cladding's boundary and its surroundings [4–6]. Although this approach greatly simplifies the retrieval of acoustic impedance, the mechanical strength of the sensing fiber is nonetheless compromised. In this work, we use a commercially available 20-m-long 80-µm-diameter single-mode silica optical fiber coated with a 8-µm-thick polyimide layer (Fig. 1) to demonstrate acoustic impedance sensing of ethanol and water. A recent parallel attempt by [10] has shown similar FSBS spectral broadening in liquids, but the mathematical retrieval of their acoustic impedances is not presented. The thin polyimide layer allows the transverse acoustic waves to traverse between the cladding boundary and the coating boundary with much reduced loss, so that the acoustic waves keep sufficient energy to complete the transverse cavity round trip. In analysis, since the acoustic impedances of fiber material and polyimide are different, the polyimide coating is treated as a thin layer that is sandwiched between the fiber and surrounding material, in good analogy with an optical thin film. Besides, polyimide-coated fiber shows excellent mechanical strength, known to sustain high temperature, and has been deployed extensively

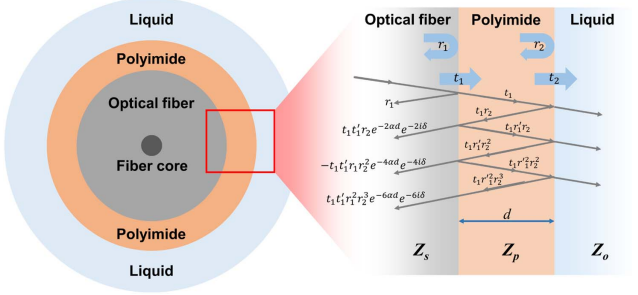

Fig. 1. Schematic diagram of the optical fiber with polyimide coating layer that acts as a 1D acoustic thin film. The reflection is angled for illustration purposes, and the transverse acoustic wave is assumed to be reflected normally from the surfaces.

as downhole sensors. As such, this work has strong potential to be adapted in the fiber optics sensing industry.

An optical fiber has a cylindrical structure that supports longitudinal, radial, torsional, and flexural acoustic vibrations that can be stimulated through electrostriction [7]. The acoustic vibrations present in the forward-scattered lights are the radial and torsional modes, which correspond to the acoustic waves that propagate transversally and circumferentially, respectively. We use the radial modes in this work as they provide the strongest response for detection. The eigenfrequencies of the radial modes for a 80-μm-diameter fiber can be calculated analytically by finding the solutions satisfying the characteristic equation of the radial transverse acoustic modes of a cylindrical waveguide [7]. In this work, we select one of the strongest modes (ninth mode, $\nu_{res} = 636$ MHz) for the sensing demonstration.

Through FSBS, two copropagating lights of frequencies ω_1 and ω_2 couple to the transverse acoustic mode of frequency $\Omega = \Delta\omega = \omega_1 - \omega_2$. Conservation of momentum requires that the axial wave vector of the acoustic wave and the copropagating lights satisfy the phase-matching condition, $K(\Omega) = k_1(\omega_1) - k_2(\omega_2)$. Since the transverse acoustic waves have negligible axial group velocity for a nearly zero axial wave vector, the phase-matching condition is relaxed, and thus the transverse acoustic waves can be stimulated over a broad range of optical wavelengths. Because of the photoelastic effect, the generated transverse acoustic waves in turn perturb the refractive index of the fiber core. A probe light at any wavelength that is introduced into the fiber will be phase modulated by the transverse acoustic waves. As such, the FSBS response impacts on the probe light as phase shifts, which can then be retrieved by using an interferometry setup that converts the induced phase shifts into intensity changes for detection [7,11]. Here, we use a Sagnac interferometer to probe the transverse acoustic waves that are stimulated by two copropagating light waves with frequency separation given by the sweeping frequency ν_F [5]. The FSBS spectrum of the polyimide-coated 80-μm-diameter fiber is shown in Fig. 2.

The FSBS spectrum obtained from the experiment (Fig. 2) exhibits multiple resonant peaks that could be individually associated to one of the calculated FSBS resonances in the 80-μm-diameter bulk fiber (Table 1). This polyimide-coated fiber has an acoustic round trip frequency in the polyimide layer,

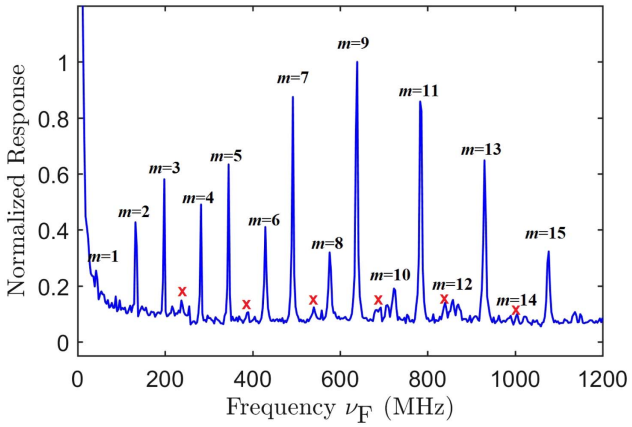

Fig. 2. FSBS spectrogram of the 80-μm-diameter polyimide-coated fiber that is measured using the frequency-sweeping technique described in [5].

Table 1. Frequencies of Resonant Modes of the 80-μm-Diameter Polyimide-Coated Optical Fiber

m	Calculation (MHz)	Measurement (MHz)
1	57	45
2	131	132
3	205	198
4	279	282
5	354	345
6	428	429
7	502	492
8	576	576
9	651	636
10	725	723
11	800	786
12	874	870
13	948	930
14	1023	1023
15	1097	1077

which is approximately twice as much as that of the silica bulk, causing the even-order modes in the polyimide layer to interfere destructively with the acoustic resonances in the bulk fiber, thus displaying reduced contrast. The resonance responses in Fig. 2 can be interpreted using the common knowledge on thin-film optical coatings: the polyimide coating thickness makes the even-order silica resonances roughly correspond to a quarter-wave propagation through the layer like an antireflection optical coating. In this case, the acoustic impedance contrast at the boundary of fiber bulk increases greatly, and the reflected acoustic wave is π-phase shifted, cancelling the incident acoustic wave and leading to the much-attenuated resonance intensity. On the contrary, the odd-order resonances, which approximately match a half-wave propagation through the coating, manifest as a replication of the impedance at the interface and make the presence of the coating acoustically imperceptible. In other words, by a slight adjustment of the coating thickness, its impact can be much reduced and ideally made inexistent. The analogy with the optical coating brings clear insight for a simple interpretation. However, unlike optical waves, the acoustic impedance does not depend on the wave velocity alone, but relies equally on the material density and compressive properties. Due to the added coupled cavity formed by the thin polyimide layer, the odd-order resonances are partially detuned and act as a strongly dispersive element.

The dynamics of transverse acoustic waves inside the polyimide-coated fiber can be simplified as a two-tier process where the acoustic impedance of the external material first affects the global acoustic reflectance of the polyimide coating layer, which in turn changes the FSBS spectral linewidth in the silica fiber structure. In other words, the linewidth broadening of FSBS resonance $\Delta\nu_m$ is considered as due to the effective reflectance R at the silica–polyimide boundary as seen by the resonating acoustic waves inside the silica fiber [4,5], given in Eq. (1). This is a simplified mathematical model that is valid only for higher order acoustic modes ($m \geq 5$), for which the acoustic wavelengths are small as compared to the size of optical fiber, and the acoustic waves are assumed as normal incident plane waves at the fiber boundary.

$$\Delta\nu_m = \Delta\nu_s - \frac{\Delta\nu_{rt}}{\pi} \ln(R), \tag{1}$$

where $\Delta\nu_{rt}$ is the round trip frequency of the transverse acoustic wave, written as $\Delta\nu_{rt} \approx V_s/2a$, where V_s is the speed of sound in silica (5950 m/s) and a is the fiber radius (40 μm); therefore, $\Delta\nu_{rt}$ for this fiber is 74 MHz. The broadening due to the intrinsic loss of the fiber material $\Delta\nu_s$ is a constant that is much smaller as compared to $\Delta\nu_m$, which can be deduced from [4] by assuming that silica has the same acoustic quality factors for the same frequency region, which gives $\Delta\nu_s \approx 0.35$ MHz at 636 MHz.

The acoustic structure of the fiber and the polyimide coating can be approximated as a 1D acoustic layer in between two bulk materials (silica and the surrounding liquids), illustrated in Fig. 1. The mathematical description of this acoustic structure is similar to an optical thin film [12]. The acoustic impedance of the structure decreases successively following this order: silica–polyimide–exterior. The acoustic impedances of silica and polyimide are $Z_s = 13.1 \times 10^6$ kg/(m^2 s) and $Z_p = 3.6 \times 10^6$ kg/(m^2 s), respectively [13], whereas the acoustic impedances of most liquids-under-test Z_o fall below 2×10^6 kg/(m^2 s). Energy is assumed to be conserved for the reflection and transmission at the interfaces. The acoustic field reflectance of silica–polyimide and polyimide–exterior boundaries, r_1 and r_2, respectively, are expressed as

$$r_1 = \left|\frac{Z_s - Z_p}{Z_s + Z_p}\right|, \qquad r_2 = \left|\frac{Z_p - Z_o}{Z_p + Z_o}\right|. \tag{2}$$

r_1 is calculated to be 0.5678. Assuming that the acoustic losses at the two boundaries are much smaller than the acoustic propagation loss inside the polyimide layer, the absolute values of r_1 and r_2 are considered in the analysis. The total field reflectance R as seen by the acoustic waves at the silica–polyimide boundary can be derived from the superposition of successive reflected waves, and the terms are in geometric series, expressed as

$$\begin{aligned} R &= r_1 + t_1 t_1' r_2 e^{-2\alpha d} e^{-2i\delta} - t_1 t_1' r_2^2 e^{-4\alpha d} e^{-4i\delta} + \ldots \\ &= \frac{r_1 + r_2 e^{-2\alpha d} e^{-2i\delta}}{1 + r_1 r_2 e^{-2\alpha d} e^{-2i\delta}}. \end{aligned} \tag{3}$$

Both t_1 and t_1' are the transmittances from silica to polyimide and vice versa, respectively, and they are related by $t_1 t_1' = 1 - r_1^2$. α is the acoustic attenuation constant of polyimide, and δ is the phase delay as the acoustic waves propagate through the polyimide layer, given as

$$\delta = \frac{2\pi\nu_{res}}{V_p} d. \tag{4}$$

ν_{res} is the resonant frequency of the transverse acoustic mode (636 MHz), V_p is the speed of sound in polyimide (2440 m/s [13]), and d is the thickness of the polyimide layer, which can be retrieved accurately from the FSBS spectrum in Fig. 2, where the small peaks marked by red crosses are due to the leakages from the acoustic resonances inside the polyimide layer. The frequency separation between the peaks is 151.7 MHz, which gives $d = 8.04$ μm. δ is then calculated to be 13.17 rad. Since R is a complex quantity where its argument (phase) is absent in the linewidth $\Delta\nu_m$ measurement, the intensity reflectance R_P should be used in the following analysis:

$$R_P = R^2 = \frac{r_1^2 + 2\eta r_1 r_2 \cos(2\delta) + \eta^2 r_2^2}{1 + 2\eta r_1 r_2 \cos(2\delta) + \eta^2 r_1^2 r_2^2}. \tag{5}$$

Here, the polyimide attenuation is written as a power ratio $\eta = \exp(-2\alpha d)$ for the ease of the subsequent algebraic manipulations.

The polyimide layer acts as a buffer for a fraction of resonating transverse acoustic waves, and thus its intrinsic acoustic loss becomes a significant factor that contributes to the FSBS linewidth broadening. The attenuation constant can nevertheless be determined in the condition where the polyimide-coated fiber is surrounded by air. In this case, $r_2 \approx 1$, Eq. (5) can then be rewritten as

$$\eta^2(R_P r_1^2 - 1) + 2\eta r_1(R_P - 1)\cos(2\delta) + R_P - r_1^2 = 0. \tag{6}$$

As R_P is obtained from Eq. (1) using the measured linewidth $\Delta\nu_m$ of air surroundings, η can be calculated by solving the quadratic equation Eq. (6) and considering only the positive solution. The measured FSBS spectrum around the resonant peak (636 MHz) with air as exterior is shown in Fig. 3(a), which is fitted with a Lorentzian function and gives $\Delta\nu_m = 2.825$ MHz. Then, η, α, and the quality factor Q are calculated to be 0.874, 8.34×10^3 m^{-1}, and 196, respectively. The measured quality factor agrees with that of the reported polyimide

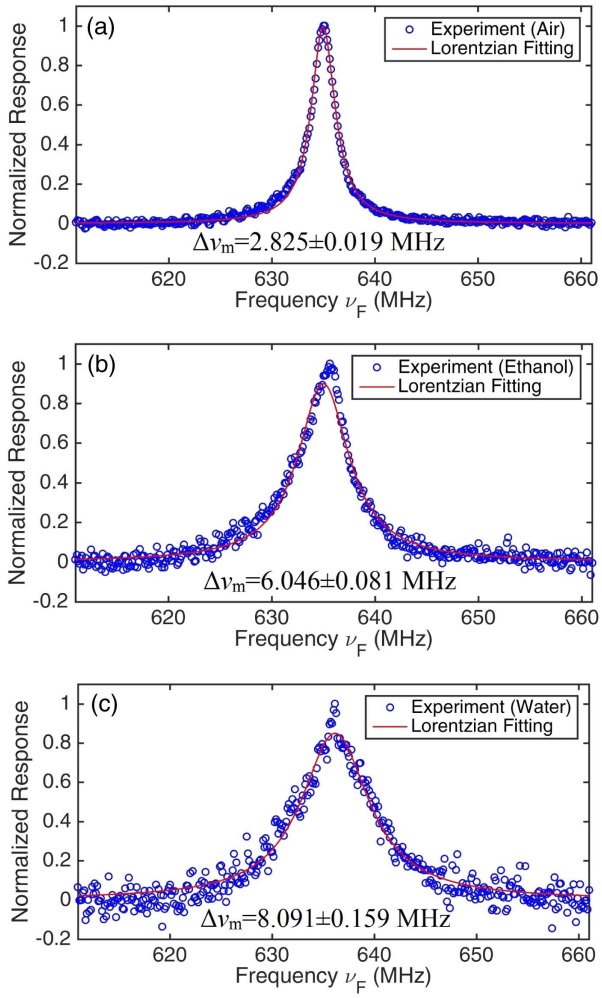

Fig. 3. Measured FSBS spectra around the selected resonant mode (636 MHz) when the polyimide-coated fiber is immersed in (a) air, (b) ethanol, and (c) water to obtain their respective acoustic impedances.

Table 2. Experimental Results and Calculations of Acoustic Impedances

Material	Ethanol	Water
$\Delta\nu_m$ (MHz)	6.046 ± 0.081	8.091 ± 0.159
R_P	0.6164 ± 0.0042	0.5182 ± 0.0070
r_2	0.5915 ± 0.0073	0.4373 ± 0.0099
Z_o ($\times 10^6$ kg/(m^2 s))	0.927 ± 0.017	1.414 ± 0.027
Standard values [13]	0.93	1.483
Mea. error, e	0.3%	4.7%

film ($Q = 200$), which was spin-coated on a silicon substrate, cured at 325°C, and characterized with an electronic transducer [14].

The measurement of acoustic impedance is demonstrated by immersing the polyimide-coated fiber into the sample liquids. The FSBS spectra around the resonant peak (636 MHz) for ethanol and water surroundings are shown in Figs. 3(b) and 3(c), respectively. In the presence of liquids, the resonant linewidth $\Delta\nu_m$ broadens, and the peak amplitude decreases. $\Delta\nu_m$ is retrieved through Lorentzian function fitting and used to calculate R_P by using Eq. (1). To obtain r_2, Eq. (5) should be rewritten as

$$r_2^2\eta^2(R_P r_1^2 - 1) + 2\eta r_1 r_2(R_P - 1)\cos(2\delta) + R_P - r_1^2 = 0. \quad (7)$$

r_2 is obtained by solving the quadratic equation Eq. (7), and only the positive solution is considered. The acoustic impedance of the surrounding liquid Z_o is subsequently calculated from Eq. (2). The experimental results and calculations are listed in Table 2.

A technique to accurately retrieve the acoustic impedances of liquids surrounding a polyimide-coated fiber is presented in this work, eliminating the need to strip away the protection coating so as to retain the mechanical strength of the sensing fiber. The measurement results of liquid acoustic impedances have less than 5% error as compared to the standard values. Although polyimide is known to swell in the presence of water vapor, the result presented here is not affected as the humidity response time of polyimide is more than 15 min [15], whereas the typical measurement time using this technique is a few seconds. The presented analysis is not limited to polyimide coating and can be used in the same way for an optical fiber coated with other materials as a thin layer, ideally with an acoustic impedance matching that of silica, being poorly hydrophilic and with a much-reduced acoustic loss. The commercial 8 μm polyimide-coated fiber turns out to provide a good response, but the best sensing properties based on this principle would require a dedicated fibre with a coating material and thickness optimized for the response. In brief, this demonstration highlights the feasibility of using a thinly coated optical fiber for acoustic impedance sensing with the considerations of practical handling as well as for the implementation of long-distance distributed measurement.

Funding. Swiss National Science Foundation (SNF) (200021L_157132).

REFERENCES

1. T. Horiguchi, K. Shimizu, T. Kurashima, M. Tateda, and Y. Koyamada, J. Lightwave Technol. **13**, 1296 (1995).
2. M. A. Soto and L. Thévenaz, Opt. Express **21**, 31347 (2013).
3. K. Hotate and T. Hasegawa, IEICE Trans. Electron. **83**, 405 (2000).
4. Y. Antman, A. Clain, Y. London, and A. Zadok, Optica **3**, 510 (2016).
5. D. M. Chow, M. A. Soto, and L. Thévenaz, in *25th Optical Fiber Sensors Conference (OFS)* (IEEE, 2017), pp. 1–4.
6. N. Hayashi, Y. Mizuno, K. Nakamura, S. Y. Set, and S. Yamashita, Opt. Express **25**, 2239 (2017).
7. R. Shelby, M. Levenson, and P. Bayer, Phys. Rev. B **31**, 5244 (1985).
8. D. M. Chow, Z. Yang, M. A. Soto, and L. Thévenaz, Nat. Commun. **9**, 2990 (2018).
9. G. Bashan, H. H. Diamandi, Y. London, E. Preter, and A. Zadok, Nat. Commun. **9**, 2991 (2018).
10. H. H. Diamandi, Y. London, G. Bashan, and A. Zadok, in *Conference on Lasers and Electro-Optics* (Optical Society of America, 2018), paper SM3K.1.
11. P. D. Townsend, A. J. Poustie, P. Hardman, and K. Blow, Opt. Lett. **21**, 333 (1996).
12. O. S. Heavens, *Optical Properties of Thin Solid Films* (Courier Corporation, 1991).
13. "Material properties tables–acoustic properties," NDT Resource Center, https://www.nde-ed.org/GeneralResources/MaterialProperties/UT/ut_matlprop_index.htm.
14. B. Hadimioglu and B. Khuri-Yakub, *Ultrasonics Symposium* (IEEE, 1990), pp. 1337–1340.
15. T. L. Yeo, T. Sun, K. T. Grattan, D. Parry, R. Lade, and B. D. Powell, IEEE Sens. J. **5**, 1082 (2005).